Neurosurgical Review
https://doi.org/10.1007/s10143-018-1023-4

ORIGINAL ARTICLE

High-resolution diffusion tensor magnetic resonance imaging of the brainstem safe entry zones

Debraj Mukherjee[1] · Veysel Antar[1] · Burcak Soylemez[1] · Ulas Cikla[1] · Bora Gürer[1] · Mehmet A. Ekici[1] · Aaron S. Field[2] · M. Shahriar Salamat[3] · Mustafa K. Başkaya[1]

Received: 27 April 2018 / Revised: 6 August 2018 / Accepted: 13 August 2018

Abstract

Operative management of intrinsic brainstem lesions remains challenging despite advances in electrophysiological monitoring, neuroimaging, and neuroanatomical knowledge. Surgical intervention in this region requires detailed knowledge of adjacent critical white matter tracts, brainstem nuclei, brainstem vessels, and risks associated with each surgical approach. Our aim was to systematically verify internal anatomy associated with each brainstem safety entry zone (BSEZ) via neuroimaging modalities commonly used in pre-operative planning, namely high-resolution magnetic resonance imaging (MRI) and diffusion tensor tractography (DTT). Twelve BSEZs were simulated in eight, formalin-fixed, cadaveric brains. Specimens then underwent radiological investigation including T2-weighted imaging and DTT using 4.7 T MRI to verify internal anatomic relationships between simulated BSEZs and adjacent critical white matter tracts and nuclei. The distance between simulated BSEZs and pre-defined, adjacent critical structures was systemically recorded. Entry points and anatomic limits on the surface of the brainstem are described for each BSEZ, along with description of potential neurological sequelae if such limits are violated. With high-resolution imaging, we verified a maximal depth for each BSEZ. The relationship between proposed safe entry corridors and adjacent critical structures within the brainstem is quantified. In combination with tissue dissection, high-resolution MR diffusion tensor imaging allows the surgeon to develop a better understanding of the internal architecture of the brainstem, particularly as related to BSEZs, prior to surgical intervention. Through a careful study of such imaging and use of optimal surgical corridors, a more accurate and safe surgery of brainstem lesions may be achieved.

Keywords Brainstem · Diffusion tensor imaging · Magnetic resonance imaging · Microsurgical anatomy · Safe entry zone · Surgical approaches

Introduction

Surgical intervention upon brainstem lesions has undergone an evolution over the last half-century. In 1969, Matson and Ingraham deemed such lesions to be inoperable [13]. In the following decades, however, series published by Lassiter et al., Epstein and McCleary, and Raimondi would demonstrate the feasibility of operating within the brainstem in select cases [6, 12, 16]. The subsequent use of microsurgical technique coupled with advances in electrophysiological monitoring and neuroimaging has led to the development of several proposed operative corridors or safe entry zones (SEZ) into the brainstem [2, 3, 8–11, 14].

In the 1990s and early 2000s, several groups published their operative series on brainstem lesions [1–3, 15, 17, 20]. Bricolo published one of the largest such series to date, detailing 175 brainstem gliomas treated through 10 specified

Debraj Mukherjee and Veysel Antar contributed equally to this work.

This manuscript has been partially reported as an oral presentation at the Congress of Neurological Surgeons Annual Meeting in September 2016 in San Diego, USA.

✉ Mustafa K. Başkaya
m.baskaya@neurosurgery.wisc.edu

[1] Department of Neurological Surgery, School of Medicine and Public Health, University of Wisconsin, CSC K4/822, 600 Highland Avenue, Madison, WI 53792, USA

[2] Department of Radiology, School of Medicine and Public Health, University of Wisconsin, Madison, WI 53792, USA

[3] Department of Pathology and Laboratory Medicine, School of Medicine and Public Health, University of Wisconsin, Madison, WI 53792, USA

Published online: 22 August 2018

brainstem safe entry zones [2]. These safe entry zones have subsequently been studied through elegant cadaveric dissection including fiber dissection techniques, detailed illustrations, and 3-dimensional photography [5, 7, 18].

In practice, use of high-resolution MRI with diffusion tensor sequences help neurosurgeons determine the operability of brainstem lesions, including delineating the lesion from normal and displaced brainstem nuclei and tracts. An understanding of these relationships, informed by cadaveric dissection but actualized through detailed study of pre-operative imaging, allows the neurosurgeon to choose the appropriate safe entry zone for each case. Nevertheless, surgical intervention for brainstem lesions often requires complex surgical approaches. These approaches regularly include significant, time-intensive skull base drilling followed by meticulous microsurgical skill within cistern spaces in order to even begin approaching the surface of the brainstem. Such technical skills leading up the brainstem portion of the operative case help avoid damage to critical cranial nerves and blood vessels, inclusive of small yet essential brainstem perforating vessels. To date, no neuroradiographic "atlas" exists to help define these critical anatomic relationships for neurosurgeons considering brainstem surgery.

In this investigation, we seek to clearly identify brainstem nuclei and tracts intimately associated with 12 brainstem safe entry zones, offering a radiographic "roadmap" to guide future neurosurgeons during their operative planning for these complex cases. We define the entry point and anatomic limits, including maximal depth, for each SEZ. We additionally describe the potential neurological sequelae if such limits are violated. The careful study of such imaging and zones may lead to more accurate and safe surgeries on brainstem lesions in the future.

Methods

Cadaveric specimen preparation

Eight (8) formaldehyde-fixed adult brains were used in this study. Brainstems were removed along with their respective cerebellums from fresh corpses who died naturally. Brainstems were then disconnected from corresponding cerebellums. Specimens with any gross lesions were excluded. Additionally, specimens belonging to patients with any neurological signs or symptoms prior to death were excluded.

Dissection of the arachnoid and surface vessels was carried out with 1 to 3 mm tipped micro-dissectors under ×6 and ×40 magnification provided by a Zeiss Surgical Microscope (Carl Zeiss AG, Oberkochen, Germany). Brainstems were fixed in 10% formaldehyde (Formalin, Sigma-Aldrich, St. Louis, USA) for 18 days. Thereafter, specimens were immersed in FC-3283 electronic liquid (Fluorinert, 3 M Electronics, St. Paul, USA), a clear, fully-fluorinated liquid used to reduce surface artifacts during MRI scanning.

Magnetic resonance diffusion tensor imaging

Each brainstem underwent initial MR diffusion tensor imaging including T2-fast-spin echo multi-slice (T2-FSEMS) imaging, diffusion-weighted imaging (DWI), and diffusion tensor tractography (DTT). These imaging modalities were repeated after operative zones were simulated using saline-saturated wooden lancets. The lancets were left in place during MR imaging to aid in making measurements between various operative zones and nearby critical structures.

All imaging was performed on a 4.7-Tesla (T), 40-cm horizontal bore scanner (Varian Inc., Palo Alto, USA) equipped with a 12-cm gradient set including a maximum gradient strength of 250 m-Telsa (mT)/meter (m).

The T2-FSEMS acquisition parameters were TR (repetition time)/TE (echo time) = 8054.16/16 ms, field of view (FOV) = 40 mm, image acquisition matrix = 256 × 256, and slice thickness = 1 mm.

DTT was acquired using a single-shot, spin-echo, echo-planar imaging sequence with diffusion-encoding gradients ($b = 1000$ s/mm) in 10 optimal encoding directions and one $b \sim 0$ reference image set. Multiple signal averages were obtained in order to maximize signal-to-noise ratio within a reasonable scan time. The diffusion tensor was estimated and tensor eigenvectors and fractional anisotropy (FA) were calculated for each voxel using standard methods. Color-coded maps of fiber tract direction were made by assigning the x-, y-, and z- directional components of the major eigenvectors to red, green, and blue color channels, respectively.

Safe entry zone simulation and measurements

Brainstem safe entry zones were simulated using saline-embedded wooden lancets with a diameter of 3 mm and with a maximum length of 2 cm (Fig. 1). Each of the 12 zones alluded to above were performed on both the left and right side of the brainstem. The entry point and anatomic limits used to define each zone are outlined in Tables 1, 2, and 3. The order in which the approaches were performed was altered for each head in order to obtain clear, representative MR diffusion tensor images for each zone.

Critical brainstem structures, including cranial nerve nuclei and fiber tracts, were identified by a blinded senior neuroradiologist (A.S.F.) and neuropathologist (M.S.S.) on initial MR imaging as well as imaging that followed safe entry zone simulation. Measurements of distance between the edge of a safe entry zone and adjacent critical structures were made in millimeters by two blinded fellows (U.C. and M.A.E.) using ImageJ (version 1.43) image processing software (National Institutes of Health, Bethesda,

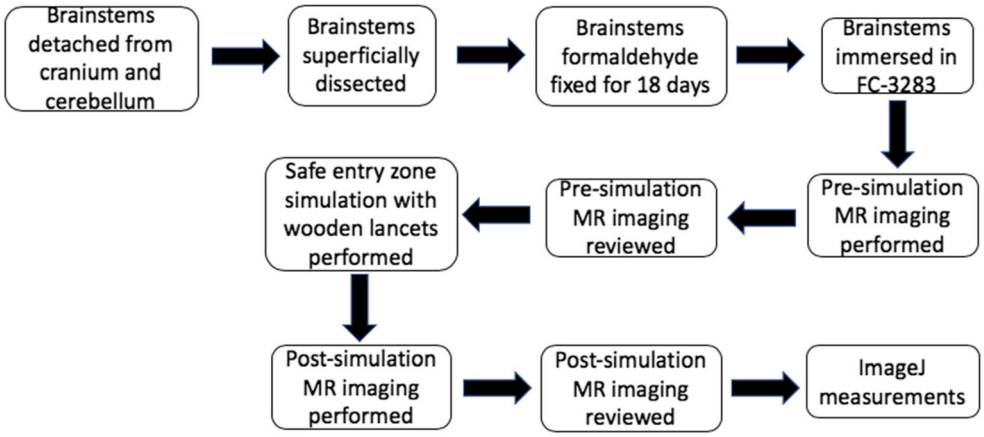

Fig. 1 Organizational chart demonstrating our methodology and workflow

USA) in the axial plane. Results were averaged between measurements made by each fellow as well as between left- and right-sided safe-entry zones.

Results

Bricolo [2, 3] has described 10 safe entry zones into the brainstem. We did not investigate Bricolo's "area acoustica," as this corridor is not widely used. Rather, we investigated two additional midbrain zones, namely the transcollicular and inferior brachial zones, as well as the ventral pontine zone, all more commonly used corridors to approach brainstem lesions. Thus, in total, we investigated 12 safe entry zones, as demonstrated in a gross specimen (Fig. 2). While these zones could be grouped into ventral/lateral/dorsal or midline/lateral categories, we grouped them based upon brainstem levels, namely the midbrain, pons, and medulla, as has been previously reported.

The midbrain contains five SEZs: supracollicular, infracollicular, transcollicular, lateral mesencephalic sulcus, and inferior brachial triangle. The pons contains four SEZs: ventral pontine, suprafacial triangle, infrafacial triangle, and median sulcus of the fourth ventricle. The medulla contains three SEZs: dorsal median sulcus, dorsal intermediate sulcus, and dorsolateral sulcus. The entry points and anatomical limits used to define BSEZs in the midbrain, pons, and medulla are outlined in Tables 1, 2, and 3, as well as further described below.

Various other nomenclatures have been used in the past to describe pontine safe entry zones. We have adopted the above nomenclature to describe the pontine safe entry zones in an attempt to provide accurate and distinctive terms for each unique zone. For clarity and consistency throughout the manuscript, we use the term "supracollicular zone" referring to the transverse dorsal incision placed just rostral to the superior colliculus of the midbrain tectum. In contrast, we use the term "suprafacial triangle" referring to the vertical paramedian dorsal incision placed within the suprafacial triangle (bordered by the facial nerve, cerebellar peduncles, and MLF) of the pons. Additionally, we use the term "infracollicular zone" referring to the transverse dorsal incision placed just caudal to the inferior colliculus of the midbrain tectum. In contrast, we use the term "infrafacial triangle" referring to the vertical paramedian dorsal incision placed within the infrafacial triangle (bordered by the medullary striae of the fourth ventricle, facial nerve, and MLF) of the pons.

Midbrain zones

Among the five primary midbrain SEZs, three zones (supracollicular, infracollicular, and transcollicular) focus on dorsally positioned lesions, while two (lateral mesencephalic sulcus and inferior brachial triangle) focus on laterally positioned lesions. Two additional BSEZs (perioculomotor/anterior mesencephalic and interpeduncular fossa) for approaching ventral lesions have been described sparingly elsewhere in the literature, but were not evaluated in this study [9].

Supracollicular

Figure 3a (T2-FSEMS) and b (DTT) demonstrate a simulated supracollicular zone in axial sections of the midbrain just rostral to superior colliculi and flanking the midline. Key radiographic landmarks, including the oculomotor nucleus, medial longitudinal fasciculus (MLF), central tegmental tract (CTT), red nucleus, medial lemniscus, substantia nigra, and cerebral peduncle, are labeled.

Average distances between the entry point of this safe entry zone and critical structures identified and measured on MR imaging are noted in Table 1. The distance from entry point to the edge of a critical structure is shortest for the oculomotor nucleus (8.3 ± 0.64 mm) and longest for the red nucleus (10.64 ± 0.48 mm).

Table 1 Midbrain safe entry zone anatomic limits and entry points by approach

Safe entry zone/approach	Neurotomy/entry point	Rostral limit	Caudal limit	Lateral limit	Medial limit	Deep limit
Supracollicular	Transverse neurotomy just rostral to the superior colliculus (unilateral or bilateral)	Posterior commissure	Rostal edge of the superior colliculus	Superior brachium	Midline (if attempting a unilateral approach)	Cerebral aqueduct (medial) and red nucleus (lateral)
Infracollicular	Transverse neurotomy just caudal to the inferior colliculus (unilateral or bilateral)	Caudal edge of the inferior colliculus	Fourth cranial nerve	Lemniscal trigone/Reil's trigone (containing the acoustic fasciculus)	Midline (if attempting a unilateral approach)	Cerebral aqueduct (medial) and red nucleus (lateral)
Transcollicular	Vertical neurotomy unilaterally through the superior and/or inferior colliculus	Posterior commissure	Fourth cranial nerve	Pulvinar and medial geniculate body	Midline (if attempting a unilateral approach)	Cerebral aqueduct (medial) and red nucleus (lateral)
Lateral mesencephalic sulcus	Oblique neurotomy along the sulcus	Medial geniculate body	Pontomesencephalic sulcus	Cerebral peduncle	Medial lemniscus (rostral) and lateral lemniscus (caudal)	Third cranial nerve crossing from red nucleus to substantia nigra (medial) and substantia nigra (lateral)
Inferior brachial triangle	Within the inferior brachium	Inferior edge of superior brachium	Fourth cranial nerve	Lateral edge of inferior brachium (superficial) and spinothalamic tract approximated by the medial lemniscus/lateral mesencephalic sulcus (deep)	Lateral edge of inferior colliculus	Fourth cranial nerve

Table 2 Pontine safe entry zone anatomic limits and entry points by approach

Safe entry zone/approach	Neurotomy/entry point	Rostral limit	Caudal limit	Lateral limit	Medial limit	Deep limit
Anterior pontine	Horizontal neurotomy just medial to the fifth cranial nerve root entry zone	Imaginary line between the lateral edge of the crus cerebri and the lateral edge of the intersection of the medullary pyramid with the pontomedullary sulcus	Pontomedullary sulcus	Fifth cranial nerve root entry zone	CST	Fifth cranial nerve motor nucleus
Suprafacial triangle	Vertical paramedian neurotomy just rostral to the facial colliculus on the floor of the fourth ventricle	Frenulum veli (containing the passing Fourth cranial nerve)	Upper facial colliculus/superior intrapontine segment of the seventh cranial nerve	Sulcus limitans	MLF (parallel and just lateral to the median sulcus of the fourth ventricle)	Motor and sensory nuclei of the fifth cranial nerve
Infrafacial triangle	Vertical paramedian neurotomy just caudal to the facial colliculus on the floor of the fourth ventricle	Facial colliculus	Medullary striae of the fourth ventricle (containing traversing segments of the eigth cranial nerve)	Seventh cranial nerve	MLF	Seventh cranial nerve, medial lemniscus, and CST
Median sulcus of the fourth ventricle	Vertical midline neurotomy just rostral to the facial colliculus	Third and fourth cranial nerve nuclei	Facial colliculus	MLF	N/A (midline incision)	Pontocerebellar fibers

CST corticospinal tract, *MLF* medial longitudinal fasciculus

Infracollicular zone

Figure 3c (T2-FSEMS) and d (DTT) demonstrate a simulated infracollicular zone in axial sections of the midbrain at the level just caudal to inferior colliculi. Key radiographic landmarks including the trochlear nucleus, lateral spinothalamic tract (STT), and tectospinal tract (TST) are labeled.

Average distances between the entry point of this safe entry zone and critical structures identified and measured on MR imaging are noted in Table 1. The distance from entry point to the edge of a critical structure is shortest for the trochlear nucleus (0.91 ± 0.17 mm) and longest for the STT (7.88 ± 0.71 mm).

Transcollicular zone

Figure 3e (T2-FSEMS) and f (DTT) demonstrate a simulated transcollicular zone in axial sections of the midbrain at a level just between the superior and inferior colliculi, but closer to the rostral edge of the inferior colliculi. Key radiographic landmarks including the trochlear nucleus, MLF, and decussation of the superior cerebellar peduncle (SCP) are labeled.

Given that the transcollicular zone as described in this study is a combination of and extension between the supracollicular and infracollicular zones, the average distance between the entry point of this safe entry zone and nearby critical structures can be inferred from the distances listed for the supracollicular and infracollicular zones as stated in Table 1.

Lateral midbrain zones

Lateral mesencephalic sulcus

Figure 3g (T2-FSEMS) and h (DTT) demonstrate a simulated lateral mesencephalic sulcus zone in axial sections of the midbrain at the level between the superior and inferior colliculi, but closer to the rostral edge of the inferior colliculi. Key radiographic landmarks including the trochlear nucleus, substantia nigra, SCP, medial lemniscus, and CTT are labeled.

Average distances between the entry point of this safe entry zone and critical structures identified and measured on MR imaging are noted in Table 1. The distance from entry point to the edge of a critical structure is shortest for the medial lemniscus (1.71 ± 0.56 mm) and longest for the fibers of the oculomotor nerve (9.32 ± 0.78 mm).

Inferior brachial triangle zone

Figure 3i (T2-FSEMS) and j (DTT) demonstrate a simulated inferior brachial triangle zone, through the brachium of the inferior colliculus, in axial sections of caudal midbrain. Key radiographic landmarks including the inferior colliculus, its

Table 3 Medullary safe entry zone anatomic limits and entry points by approach

Safe entry zone/approach	Neurotomy/entry point	Rostral limit	Lateral limit	Medial limit	Deep limit
Posterior median sulcus of the medulla	Vertical midline incision just caudal to obex	Obex	Medial edge of fasciculus gracile	N/A (midline incision)	12th cranial nerve nucleus
Posterior intermediate sulcus	Vertical midline incision along just caudal to clava	Clava	Medial edge of fasciculus cuneate	Lateral edge of fasciculus gracile	Solitary tract
Posterior lateral sulcus	Vertical midline incision just caudal to	Tuberculum cuneatum	Inferior cerebellar peduncle	Lateral edge of fasciculus cuneate	Trigeminal spinal tract

N/A not applicable

brachium, periaqueductal gray, CTT, medial lemniscus, MLF, decussation of the SCP, substantia nigra, and cerebral peduncle are labeled.

Average distances between the entry point of this safe entry zone and critical structures identified and measured on MR imaging are noted in Table 1. The distance from a surface entry point to the edge of a critical structure is shortest for the trochlear nucelus (3.13 ± 0.47 mm) and longest for the medial lemniscus (8.64 ± 0.49 mm).

Pontine zones

Among the four primary pontine safe entry zones, one focuses on ventral pathology (ventral pontine zone), while three others focus on dorsal pathology (suprafacial triangle, infrafacial triangle, and median sulcus of the 4th ventricle). Three additional safe entry zones (supratrigeminal, infratrigeminal, and superior fovea triangle) for lateral approaches to potential pontine pathology have been described elsewhere in the literature, but these zones are not evaluated in this study [5, 19].

Ventral pontine zone

Figure 4a (T2-FSEMS) and b (DTT) demonstrate a simulated ventral pontine zone in axial sections of the pons at the level of the abducens nucleus. Key radiographic landmarks including the abducens nucleus, fibers of the facial nerve, and corticospinal tract (CST) fibers are labeled.

Average distance between entry point and critical structures identified and measured on MR imaging is noted in Table 2. The distance from entry point to edge of a critical structure is shortest for the CST fibers (5.43 + 1.78 mm).

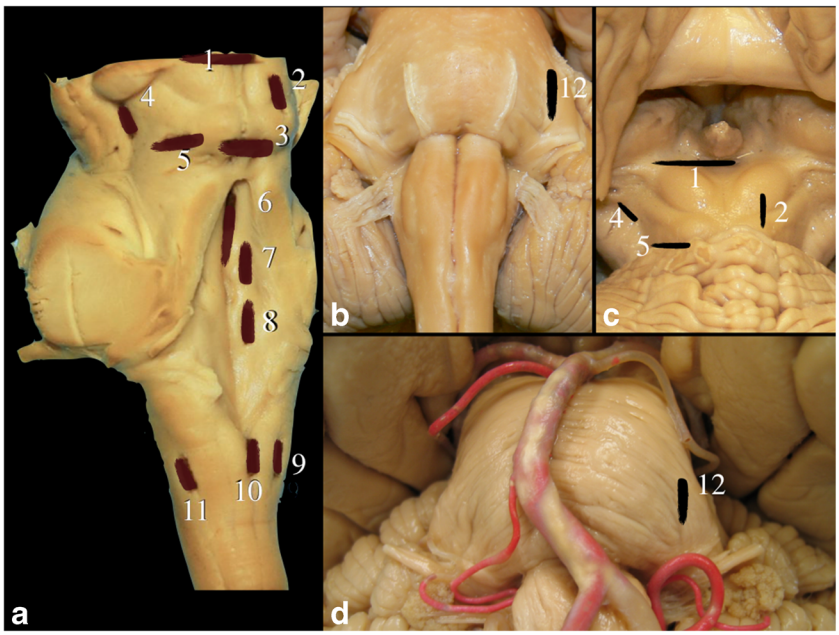

Fig. 2 Illustration of the brainstem safe entry zones studied in this study. **a** Posterolateral and **b** anterior views human cadaveric brain stems. **c** Posterior supracerebellar view of brain stem with upper vermis, splenium, and pineal gland. **d** Anterior view of the brain stem with posterior circulation arteries, brain, and cerebellum. Entry points representing 12 brainstem safe entry zones have been marked and numbered on the specimen including (1) supracollicular, (2) transcollicular, (3) infracollicular, (4) lateral mesencephalic sulcus, (5) inferior brachial triangle, (6) median sulcus of the fourth ventricle, (7) suprafacial triangle, (8) infrafacial triangle, (9) dorsal intermediate sulcus, (10) dorsal median sulcus of the medulla (11) dorsolateral sulcus, and (12) ventral pontine zones

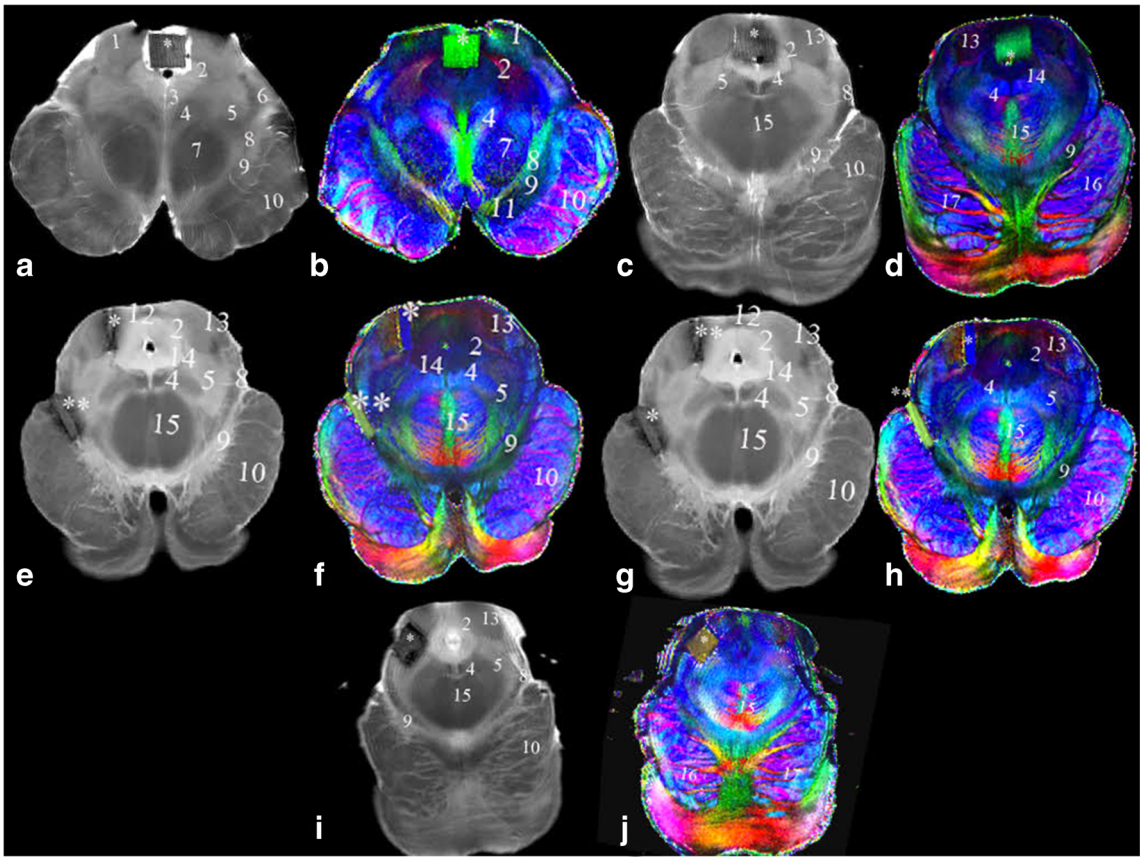

Fig. 3 MR imaging including T2-FSEMS sequences (**a**, **c**, **e**, **g**, **i**) and directionally-encoded DTT (**b**, **d**, **f**, **h**, **j**) was conducted on human midbrain cadaveric specimens using a 4.7 T machine to better understand the internal architecture of normal brainstem structures as related to 5 *midbrain* safe entry zones, namely the supracollicular (**a**–**b**), infracollicular (**c**–**d**), transcollicular (**e**–**f**), lateral mesencephalic sulcus (**g**–**h**), and inferior brachial triangle (**i**–**j**) zones. 1: nucleus of the superior colliculus; 2: periaqueductal gray matter, 3:occulomotor nucleus; 4: medial longitudinal fascicle; 5: central tegmental tract; 6: lateral spinothalamic tract; 7: red nucleus; 8:medial lemniscus; 9: substantia nigra; 10: crus cerebri; 11: fibers of the third cranial nerve; 12: commissure of the inferior colliculus; 13: nucleus of the inferior colliculus; 14: trochlear nucleus; 15: decussiation of the superior cerebellar pedincle; 16: corticospinal fibers; 17: pontocerebellar fibers

Dorsal pontine zones

Suprafacial triangle

Figure 4c (T2-FSEMS) and d (DTT) demonstrate a simulated suprafacial triangle zone in axial sections of the pons at the level just rostral to the facial colliculus. Key radiographic landmarks including the MLF are labeled.

Average distance between entry point and critical structures are measured on MR imaging and noted in Table 2. The distance from entry point to the edge of a critical structure is shortest for the MLF (0.88 ± 0.13 mm) and longest for the CST fibers (13.49 ± 1.40 mm).

Infrafacial triangle

Figures 4e (T2-FSEMS) and 3f (DTT) demonstrate a simulated suprafacial triangle zone in axial sections of the pons at the level just caudal to the facial colliculus. Key radiographic landmarks including the MLF are labeled.

Average distance between entry point and critical structures are measured on MR imaging and noted in Table 2. The distance from an entry point to the edge of a critical structure is shortest for the MLF (0.70 ± 0.40 mm) and longest for the CST (13.32 ± 1.05 mm).

Median sulcus of the fourth ventricle

Figure 4g (T2-FSEMS) and h (DTT) demonstrate a simulated median sulcus of the fourth ventricle zone in axial sections of the pons at a level just rostral to the facial colliculus. Key radiographic landmarks include the MLF and transverse pontine fibers that are labeled.

Average distance between the entry point of a safe entry zone and critical structures are measured on MR imaging and noted in Table 2. The distance from entry point to the edge of a critical structure is shortest for the MLF (1.71 ± 0.22 mm) and longest for CST (13.59 ± 1.29 mm).

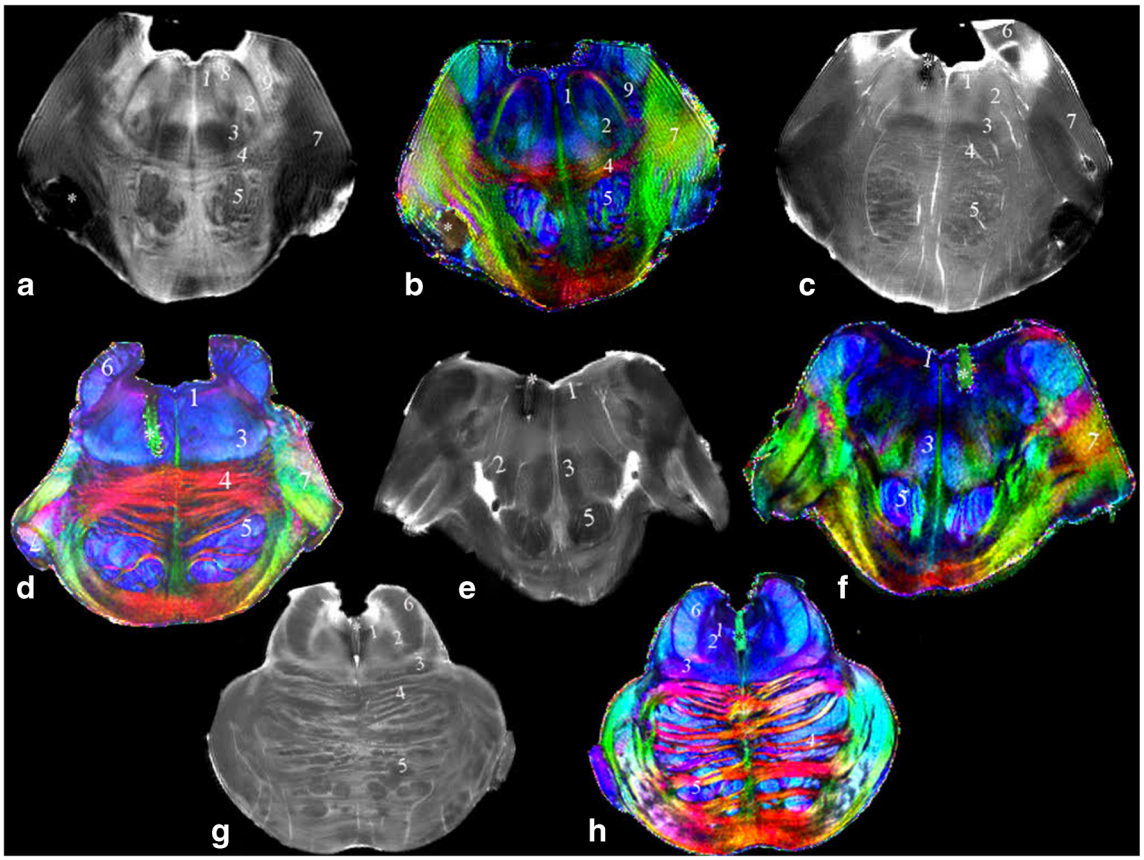

Fig. 4 MR imaging including T2-FSEMS sequences (**a**, **c**, **e**, **g**) and directionally-encoded DTT (**b**, **d**, **f**, **h**) was conducted on human pons cadaveric specimens using a 4.7 T machine to better understand the internal architecture of normal brainstem structures as related to 4 *pontine* safe entry zones, namely the ventral pontine zone (**a**–**b**), supra facial triangle (**c**–**d**), infra facial triangle (**e**–**f**), and median sulcus of the fourth ventricle (**g**–**h**) zones. 1: medial longitudinal fascicle; 2: central tegmental tract; 3: medial lemniscus; 4: pontocerebellar fibers; 5: cerebrospinal fibers; 6: superior cerebellar pedincle; 7: middle cerebellar pedincle; 8: abducens nerve; 9: facial nerve fibers

Medulla

While safe entry zones in the midbrain and pons are traditionally described in subdivisions based upon their ventral, dorsal, or lateral entry point, most studies of medullary safe entry zones do not rigorously employ this subdivision schema. As a result, we have not employed the subdivision schema to categorize the dorsal medullary safe entry zones described in this study.

Three (3) primary dorsal medullary safe entry zones have been described, namely the dorsal median sulcus zone, dorsal intermediate sulcus, and dorsolateral sulcus zones. Additionally, four ventrolateral safe entry zones for approaching the ventral medulla have been described, but are not evaluated in this study [5]. For reference, these ventrolateral medullary zones include the ventrolateral sulcus/preolivary, olivary, retroolivary/postolivary, and lateral medullary/inferior cerebellar peduncle zones.

Figure 5a (T2-FSEMS) and b (DTT) demonstrate simulated dorsal median, dorsal intermediate, and dorsolateral sulcus zones in axial sections of the medulla at the level just caudal to the inferior olive. Key radiographic landmarks including the nucleus gracilis, nucleus cuneatus, and pyramidal decussation are labeled.

Average distance between the entry point of a safe entry zone and critical structures are measured on MR imaging and noted in Table 3. The distance from the dorsal median sulcus zone of the medulla entry point to the hypoglossal nucleus is 4.31 + 0.71 mm. The distance from the dorsal intermediate sulcus entry point to the lateral corticospinal tract is 5.10 + 0.82 mm. The distance from the dorsolateral sulcus entry point to the pyramidal decussation is 5.27 + 1.30 mm.

Discussion

Once thought to be universally inoperable, selective lesions of the brainstem are now amenable to surgery by experienced surgeons with adjunct microsurgical instruments, high-quality pre-operative imaging, intra-operative image guidance and monitoring, neurointensive care support, and intricate knowledge of brainstem safe entry zones. In the more recent past, cadaveric series have attempted to describe the microsurgical anatomy of brainstem safe entry zones in detail [12].

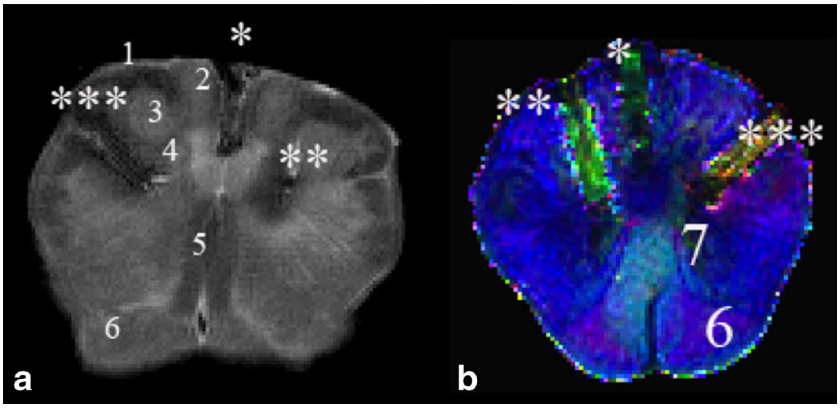

Fig. 5 MR imaging including an T2-FSEMS sequence (**a**) and directionally-encoded DTT (**b**) was conducted on a human medulla cadaveric specimen using a 4.7 T machine to better understand the internal architecture of normal brainstem structures as related to 3 dorsal *medullary* safe entry zones, namely the dorsal median sulcus of the medulla, dorsal intermediate sulcus, and dorsolateral sulcus zones. Simulated posterior median sulcus (*), posterior intermediate sulcus (**), and posterior lateral sulcus (***) safe entry zones to the medulla oblongata. 1: fasciculus gracilis; 2: fasiculus cuneatus; 3: nucleus gracilis; 4: nucleus cuneatus; 5:medial lemniscus; 6: pyramid; 7: dessuciation of the pyramid

Although several series have described some additional zones, the 10 brainstem safe entry zones described by Bricolo [2, 3] have represented a relatively widely accepted set of basic approaches to the brainstem. In an effort to better understand the internal architecture of the brainstem as related to each of these brainstem safe entry zones, we have used high-resolution MRI and DTT methods in this study. All approaches generally adhere to the two-point rule, representing the shortest distance between entry point and target while minimizing injury to critical centers and avoiding perforators [4].

Midbrain

Dorsal midbrain zones

Supracollicular zone

The supracollicular zone is often used for lesions of the tectum, utilizing a suboccipital craniotomy with a subsequent supracerebellar-infratentorial approach (or one of its many variants) to advance toward the lesion.

Inferior extension of the incision into the superior colliculus may cause deficits of the voluntary component of rapid eye movements and difficulty coordinating movements of the head and eyes. When possible, only a unilateral incision is made to avoid post-operative visual disturbances. The posterior commissure is avoided rostrally to minimize risk dorsal midbrain syndrome. Transgressing the cerebral aqueduct at the medial depth of this zone may damage the more ventral oculomotor nucleus and MLF, resulting in a possible third nerve palsy and internuclear ophthalmoplegia, respectively. Transgressing the cerebral aqueduct at the lateral depth of this zone risks injury to the red nucleus, with possible post-operative tremor, abnormal muscle tone, or choreoathetosis. Further extension of deep and lateral may injure, from medial to lateral, the trigeminal mesencephalic nucleus and tract, CTT, and red nucleus, resulting in altered sensation/motor function to the face, palatal myoclonus, and abnormal tremor/muscle tone/choreoathetosis, respectively.

Based upon our anatomic study, the deficits most at risk following a supracollicular approach for a tectal lesion would include third nerve palsy and tremor/abnormal muscle tone/choreoathetosis from injury to the oculomotor nucleus and red nucleus, respectively.

Infracollicular zone

The infracollicular zone is also used for lesions of the tectum, utilizing a suboccipital craniotomy with a subsequent supracerebellar-infratentorial approach (or one of its many variants) to advance toward the lesion.

Rostral extension of the incision into the inferior colliculus may impact auditory perception. When possible, only a unilateral incision is made to avoid post-operative auditory disturbances. Transgressing the cerebral aqueduct at the medial depth of this zone may damage the more ventral trochlear nucleus, MLF, and decussating superior cerebellar peduncle, resulting in fourth nerve palsy, internuclear ophthalmoplegia, and bilateral cerebellar signs, respectively. Transgressing the cerebral aqueduct at the lateral depth of this zone risks injury to the red nucleus. Extension of the entry laterally into the lemniscal trigone may injure the acoustic fasciculus, causing cortical deafness. Extension of the entry rostral, deep, and lateral may injure structures just lateral to the cerebral aqueduct, mirror injury at the level of the superior colliculus. Extension of the entry caudal, deep, and lateral may injure structures just lateral and deep to the medial edge of the

lemniscal trigone, including the superior cerebellar peduncle and lateral lemniscus, resulting in ipsilateral cerebellar signs and decreased contralateral auditory perception, respectively.

Based upon our anatomic study, the deficits most at risk following an infracollicular approach for a tectal lesion would be trochlear nerve palsy. We recorded a distance of less than 1 mm between the edge of this safe entry zone and the trochlear nucleus. Of note, the operating microsurgeon should be particularly cognizant of avoiding the trochlear nerve itself during the surgical approach to this safe entry zone. This operative corridor is quite narrow, possibility precluding its widespread use.

Transcollicular zone

Like the supracollicular and infracollicular zones, the transcollicular zone is also used for lesions of the tectum, utilizing a suboccipital craniotomy with a subsequent supracerebellar-infratentorial approach (or one of its many variants) to advance toward the lesion. A transcollicular zone may be chosen for unilateral lesions longer in rostro-caudal dimension than could be easily approached via a supracollicular or infracollicular zone alone.

With transcollicular zones, a *vertical* incision or entry is made off midline and unilaterally through the superior colliculus, inferior colliculus, or both (Fig. 6). Visual and auditory deficits following injury to unilateral superior and inferior colliculi in pursuit of tectal lesions have been minimal in reported series but have been noted in the senior author's (MKB) own unpublished series [9] (Fig. 6). Injury to the pulvinar and medial geniculate body may manifest for rostrolateral extension beyond this safe entry zone, resulting in deficits to visual and auditory processing, respectively. Extension beyond the caudolateral limits of this zone include possible damage to the superior cerebellar peduncle and lateral lemniscus, both located just lateral and deep to the medial edge of the lemniscal trigone.

Based upon our anatomic study, the deficits most at risk following a transcollicular approach for a tectal lesion would include third nerve and fourth nerve palsies.

Lateral midbrain zones

Lateral mesencephalic sulcus zone

The lateral mesencephalic sulcus zone is used for lesions of the cerebral peduncle or tegmentum. Utilizing a suboccipital craniotomy, with either a paramedian supracerebellar-infratentorial, retrosigmoid, or retrolabyrinthine approach, the surgeon is able to angle their incision or entry either ventrally toward the cerebral peduncle or dorsally toward the tegmentum in order to reach a lesion in either location.

Extension of this incision rostrally may damage the medial geniculate body rostrally, with resultant deficits of auditory

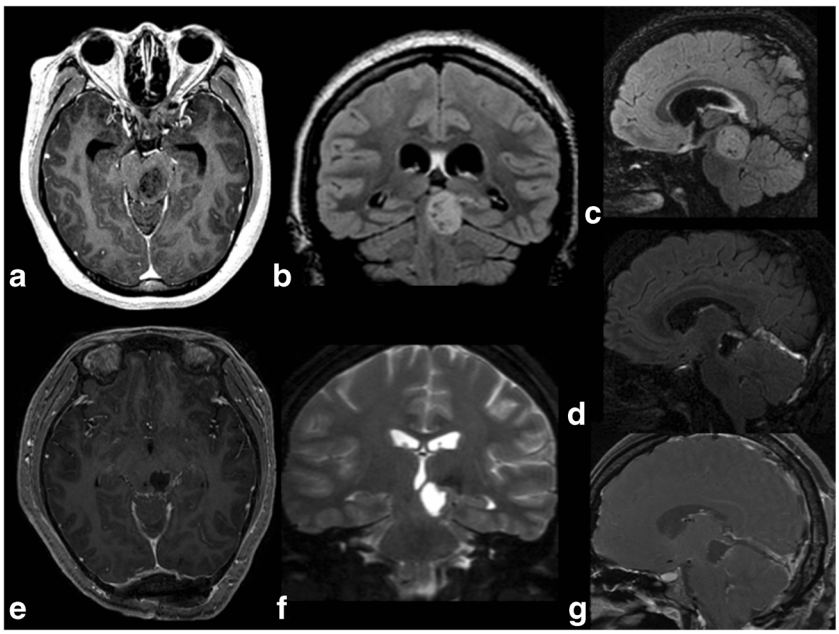

Fig. 6 Pre-operative post-contrast axial T1 (**a**), coronal T2 FLAIR (**b**), and sagittal T2 FLAIR (**c**) MR imaging of a 23-year-old female patient who presented with double vision and walking difficulty demonstrating a slightly enhancing expansile mass lesion in the midbrain. The patient underwent gross total resection of an anaplastic grade III astrocytoma via an infratentorial supracerebellar craniotomy using a transcollicular approach. Due to mass effect, the trochlear nerve was used as an anatomical landmark to localize the inferior colliculus on the left side. The vertical incision was then made in both colliculi. Post-operative non-contrast T1 sagittal (**d**), post-contrast T1 axial (**e**), T2 coronal (**f**), and post-contrast T1 sagittal (**g**) MR imaging demonstrating gross total resection of the tumor. The patient experienced worsening of her vertical diplopia for about a week after surgery. These findings improved significantly over 2 weeks

processing. To avoid a third nerve palsy, medially this zone stops just lateral to the oculomotor nerve fibers as they cross the red nucleus and the substantia nigra to exit the midbrain. Laterally, the depth of this zone is the substantia nigra in order to avoid post-operative parkinsonism. Angling the approach ventrolaterally approximates the cerebral peduncle, in which unintentional injury could lead to motor weakness from interruption of corticobulbar/corticospinal tracts. Angling the approach ventromedially approximates the medial lemniscus, in which unintentional injury could lead to contralateral somatosensory loss. Angling the approach dorsomedially approximates the lateral lemniscus, in which unintentional injury could lead to decreased contralateral auditory perception. By creating an entry through the lateral mesencephalic sulcus, perpendicular to the surface of the brainstem, the neurosurgeon approaches deeper structures within the tegmentum including, in order from lateral to medial, the TMT, CTT, red nucleus, decussation of the SCP, oculomotor nucleus, and trochlear nucleus. Care must be taken to avoid unintentional injury to these structures.

Based upon our anatomic study, the structure most at risk following a lateral mesencephalic sulcus approach is the medial lemniscus.

Inferior brachial triangle zone

The inferior brachial triangle zone is used for lesions of the lateral tectum, utilizing a suboccipital craniotomy with a paramedian supracerebellar-infratentorial approach to advance toward the lesion.

The entry is made within the bounds of the brachium of the inferior colliculus, avoiding possible rapid eye movement dysfunction from injury to the more rostral superior colliculus brachium. Preservation of the STT while accessing this safe entry zone helps maintain contralateral pain/temperature sensation.

Based upon our anatomic study, the structure most at risk following an inferior brachial triangle approach is the trochlear nerve.

Pons

Ventral pontine zone

The ventral pontine zone is used for lesions of the basal pons, utilizing an anterior petrosectomy or retrolabyrinthine approach to advance toward the lesion.

The medial border of this zone is the CST, to which injury may manifest as contralateral limb weakness, and the caudal border is the pontomedullary sulcus, to which an injury may manifest as a combination of sensory and motor deficits similar to lateral medullary syndrome. Extension beyond the rostral border of this zone into the lateral edge of the medullary pyramid may cause contralateral motor weakness and lateral medullary syndrome-like symptoms.

Based upon our anatomic study, the deficit most at risk following a ventral pontine zone approach for a basal pons lesion would be contralateral weakness from injury to the CST.

Dorsal pontine zone

Suprafacial triangle zone

The microsurgical decision to use a suprafacial versus an infrafacial triangle zone is based primarily upon the relationship of the lesion to the facial colliculus. In the operative setting, identification of the facial colliculus can be challenging. In such instances, reliance on other contextual clues, such as adjacent cranial nerves, and neuromonitoring may be particularly helpful to the surgeon.

The suprafacial triangle zone is used for lesions in the dorsal pons located rostral to the facial colliculus, utilizing a midline suboccipital craniotomy followed by either a telovelar, transvermian, or cerebellomedullary approach to advance toward the lesion.

Extension of the incision rostrally may damage the facial colliculuss, injury to which would cause ipsilateral facial paralysis and ipsilateral abducens palsy manifest as medial eye deviation. The lateral border of this triangle is the sulcus limitans, which is the lateral limit of the medial vestibular nuclei, injury to which would cause uncoordinated head and eye movements. The deep limit of this zone is the motor and principle sensory nuclei of the trigeminal nerve; injury to these structures would manifest as ipsilateral motor weakness (for instance in muscles of mastication) and decreased contralateral sensation to the face, respectively.

Based upon on our anatomic study, the deficit most at risk following a suprafacial triangle approach for a dorsal pontine lesion would be internuclear ophthalmoplegia from injury to the MLF.

Infrafacial triangle zone

The infrafacial triangle zone is used for lesions of the dorsal pons located caudal to the facial colliculus, utilizing a midline suboccipital craniotomy followed by either a telovelar, transvermian, or cerebellomedullary approach to advance toward the lesion (Fig. 7).

The entry caudally stops short of the medullary striae of the fourth ventricle, composed of nerves from the arcuate nucleus of the medulla as well as the dorsal acoustic striae of the vestibulocochlear nerve, injury to which may cause ipsilateral/contralateral/bilateral hearing loss. Further extension of the entry caudal to the stria medullaris of the fourth ventricle

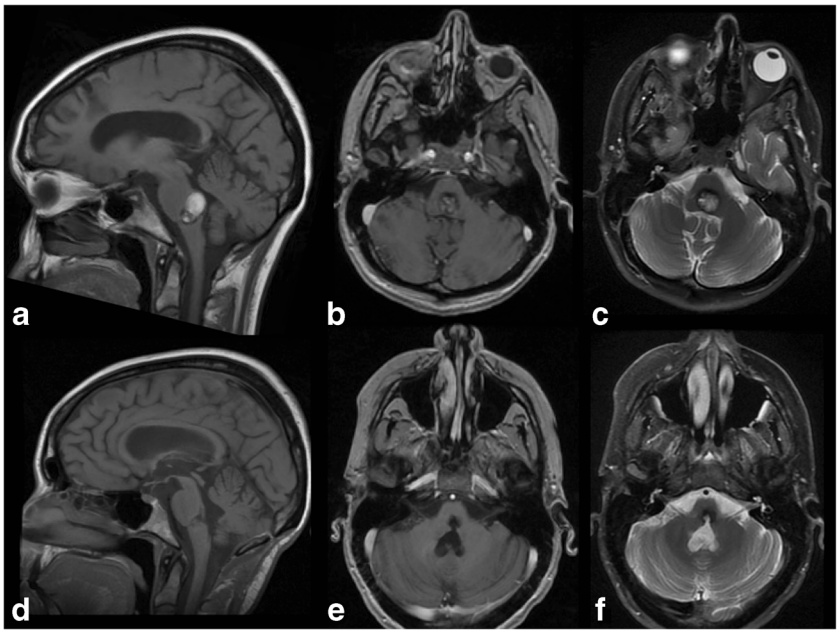

Fig. 7 Pre-operative non-contrast T1 sagittal (**a**), post-contrast T1 axial (**b**), and T2 axial (**c**) MR imaging of a 41-year-old female who presented with multiple episodes of hemorrhage demonstrating a slightly enhancing hemorrhagic lesion in the pons. The patient's last episode of hemorrhage resulted in severe deficits including internuclear ophthalmoplegia and severe truncal ataxia. The patient underwent gross total resection of a pontine cavernous angioma via a midline suboccipital craniotomy using an infrafacial approach. Mapping of the abducens and facial nerves were utilized during surgery. Post-operative non-contrast sagittal T1 (**d**), post-contrast axial T1 (**e**), and axial T2 MR imaging demonstrating gross total resection of the cavernous angioma. Although the patient showed gradual improvement of her pre-operative neurological deficits over months, she remained with mild internuclear ophthalmoplegia and moderate truncal ataxia

would enter the hypoglossal trigone, potentially causing motor weakness of the tongue. The lateral border of this triangle is marked by the tela choroidea's most medial point of attachment at the lower edge of the lateral recess. Just lateral and deep to this point of attachment lies the facial nucleus, injury to which would cause ipsilateral facial paralysis.

Based upon on our anatomic study, the deficit most at risk following an infrafacial triangle approach for a dorsal pontine lesion would be internuclear ophthalmoplegia from injury to the MLF (Fig. 7).

Median sulcus of the fourth ventricle zone

The median sulcus of the fourth ventricle zone is used for lesions of the dorsal pons, utilizing a midline suboccipital craniotomy followed by either a telovelar, transvermian, or cerebellomedullary approach to advance toward the lesion. The decision between using a suprafacial versus median sulcus of the fourth ventricle zone is based primarily upon the relationship of the lesion to the MLF, with a suprafacial zone used for lesions lateral to the MLF and a median sulcus of the fourth ventricle zone used for lesions within the small space between bilateral MLF. As a result of this very narrow indication, median sulcus of the fourth ventricle zones are rarely used in practice.

The midline vertical incision for a median sulcus of the fourth ventricle zone is made rostral to and between the projections of the abducens nuclei on the surface of the pons, taking advantage of this small area lacking crossing fibers. The lateral limit of this narrow entry is the MLF bilaterally that must be avoided to prevent post-operative internuclear ophthalmoplegia. The crossing pontocerebellar fibers represent the deep limit of this zone, injury to which would lead to post-operative bilateral cerebellar signs.

Based upon on our anatomic study, the deficit most at risk following a median sulcus approach for a dorsal pontine lesion would be internuclear ophthalmoplegia from injury to the MLF.

Medulla

The three (3) dorsal medullary zones all utilize a midline suboccipital craniotomy and C1 laminectomy for exposure. The microsurgical decision regarding which of these zones to use relates to the lesion's relationship to the nucleus gracilis, nucleus cuneatus, hypoglossal nucleus, solitary tract, and spinal trigeminal nucleus and tract. If the lesion is primarily midline and displaces the nucleus gracilis or hypoglossal nucleus laterally, then the dorsal median sulcus zone of the medulla would be preferred. If the lesion is primarily dorsolateral and displaces the nucleus cuneatus and solitary tract, then the dorsal intermediate sulcus zone would be preferred. If the lesion is centered farther laterally between the nucleus cuneatus and

solitary tract, as well as the inferior cerebellar peduncle and spinal trigeminal tract, then the dorsolateral sulcus zone would be preferred.

Of note, the dorsal median sulcus zone of the medulla is anatomically distinct from the pontine median sulcus of the fourth ventricle zone. Both zones involve midline incisions, but the median sulcus of the fourth ventricle zone extends caudally to the level of the obex, while the dorsal median sulcus zone lies caudal to the obex.

Dorsal median sulcus of the medulla zone

Rostral to this obex and flanking the midline of the caudal fourth ventricle lies the calamus scriptorius, a cardio-inhibitory center. Thus, the incision is rostrally limited by the level of the obex (Fig. 8). The entry is extended caudally as needed to allow exposure of the lesion in question. The entry may extend as deep as the hypoglossal nuclei and laterally it abuts the fasciculus gracilis, where injury may cause motor weakness of the tongue or lower limb sensory loss, respectively.

Based upon on our anatomic study, the deficit most at risk following use of the dorsal median sulcus of the medulla zone would be motor weakness of the tongue from injury to the hypoglossal nucleus.

Dorsal intermediate sulcus zone

A para-midline vertical incision is made just caudal to the clava, rostral to which lies the calamus scriptorius on the floor of the fourth ventricle. The entry is extended caudally as needed to allow exposure of the lesion in question. The entry may extend as deep as the solitary tract, medially abutting the fasciculus gracilis and laterally abutting the fasciculus cuneatus before affecting taste, lower limb sensation, or upper limb sensation, respectively.

Based upon on our anatomic study, the deficit most at risk following use of the dorsal intermediate sulcus zone would be

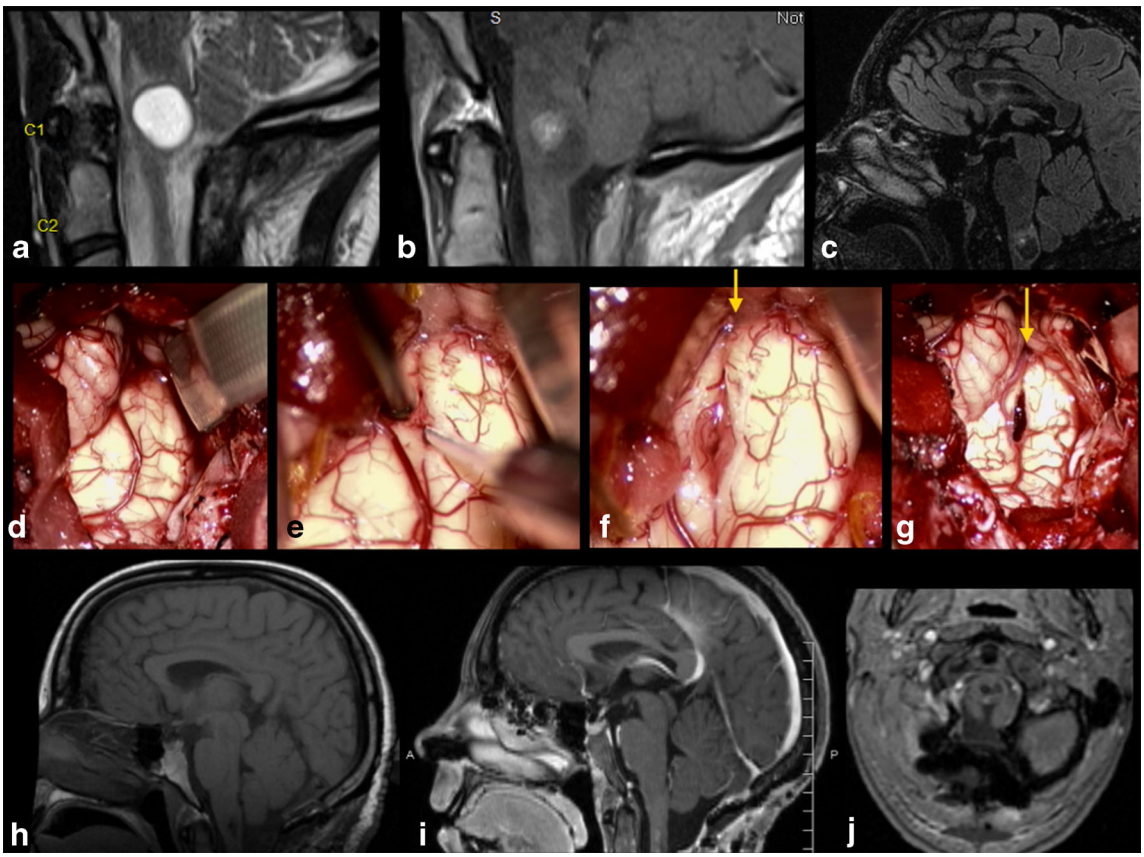

Fig. 8 Pre-operative sagittal T2 (**a**), post-contrast sagittal T1 (**b**), and non-contrast sagittal T1 (**c**) MR imaging of a 35-year-old female demonstrating a partially enhancing mass lesion in the lower medulla. This lesion was incidentally found after the patient underwent resection of a spinal cord ependymoma at another hospital and presented with progressive growth over the subsequent 2 years. The patient underwent gross total resection of a WHO grade II ependymoma via a midline suboccipital craniotomy with C1 laminectomy using a dorsal median sulcus approach (**d**, **e**, **f**, and **g**). Intraoperative pictures demonstrating the brainstem before entering into the safe entry zone (**d**), opening of the dorsal median sulcus (**e**), and view of the brainstem during (**f**) and after tumor removal (**g**) with the yellow arrow pointing toward the obex. The patient did not experience any post-operative neurological deficits. Post-operative non-contrast sagittal T1 (**h**), post-contrast sagittal T1 (**i**) and post-contrast axial T1 (**j**) MR imaging demonstrating gross total resection

motor weakness of the tongue from injury to the hypoglossal nuclei.

Dorsolateral sulcus zone

A more lateral vertical incision is made just caudal to the tuberculum cuneatum, which is the rostral-most extension of the fasciculus cuneate. The entry is extended caudally as needed to allow exposure of the lesion in question. The entry may extend as deep as the spinal trigeminal tract, medially abutting the fasciculus cuneate, or laterally abutting the inferior cerebellar peduncle before affecting ipsilateral sensation of the face, upper extremity sensation, or ipsilateral balance and hearing, respectively.

Based upon on our anatomic study, the deficit most at risk following use of the dorsal intermediate sulcus zone would be motor weakness of the tongue from injury to the hypoglossal nuclei.

Limitations

Several significant limitations affect this work. For instance, our gross cadaveric dissections did not include fiber-dissection technique, which also has its own limitations. Fiber dissection methodology has already been used by previous authors to describe these zones [16–18]. Rather, we have focused on using MR imaging and diffusion tensor tractography to illustrate the internal architecture of the brainstem as related to each safe entry zone to assist the reader in visualizing the effect of each approach upon normal architecture within the brainstem. The wooden lancets used in our simulated safe entry zones were visible on post-simulation imaging due to the diffusion of water within these lancets. While blinded fellows did not subjectively report interference from the wooden lancets during their measurements, it is possible that the lancets did produce some artifact on imaging. We are investigating alternatives to our wooden lancet methodology to decrease possible artifactual interference during future safe entry zone simulations in cadaveric specimens. Brainstem architecture is often distorted in actual operative cases, but, nevertheless, we hope this work provides a template to readers for future reference. Although we have not covered every possible brainstem safe entry zone, including the described intercollicular, perioculomotor/anterior mesencephalic, or anterolateral zones in the medulla, we hope to have provided a foundation of principles upon which the reader can rely upon in making future operative decisions regarding lesions of the brainstem [5]. Additionally, though each operative case is unique, the careful study of pre-operative imaging, intra-operative image guidance, and the judicious use of intraoperative neuromonitoring remain perhaps the greatest surgical adjuncts to sound microsurgical knowledge and experience when tackling lesions of the brainstem. Finally, this study is based upon imaging from a relatively small sample of eight cadaveric specimens. Variability exists in the size and dimensions of each human brain and thus surgical access to each brainstem safe entry zone should be individualized to each patient's unique anatomy, neuroimaging findings, pathology, and goals of care.

Conclusions

We have used high-resolution MRI and diffusion tensor tractography to perform an in-depth study of 12 common brainstem safe entry zones. This work provides visualization of internal architecture as related to each brainstem safe entry zone using commonly using pre-operative imaging modalities. This work supplements previous operative case series and cadaveric studies, hopefully making the reader more knowledgeable and comfortable in their use of such brainstem zones. The continued, careful study of such images and zones may lead to more accurate and safe operations upon the brainstem in the future.

Funding information Debraj Mukherjee, MD, MPH is partially supported by The Robert Wood Johnson Foundation, The Beckwith Institute, and an American Medical Association Foundation Seed Grant. None of these grants were used in this study.

Compliance with ethical standards

Conflict of interest The authors declare that they have no conflict of interest.

Ethical approval The complete study was performed on the cadaveric specimens of the Department of Neurosurgery, University of Wisconsin, Madison, USA. According to the Institutional Rules, the use of these cadaveric specimens for anatomical dissections does not require specific approval from ethics committee.

This article does not contain any studies with human participants or animals performed by any of the authors. For this type of study, formal consent is not required.

References

1. Abla AA, Lekovic GP, Turner JD, de Oliveira JG, Porter R, Spetzler RF (2011) Advances in the treatment and outcome of brainstem cavernous malformation surgery: a single-center case series of 300 surgically treated patients. Neurosurgery 68(2):403–415
2. Bricolo A (2000) Surgical management of intrinsic brain stem gliomas. Oper Tech Neurosurg 3(2):137–154
3. Bricolo A and Turazzi S. Surgery for gliomas and other mass lesions of the brainstem. Adv Tech Stand Neurosurg (Vol. 22, pp. 261–341). Vienna: Springer. 1995
4. Brown AP, Thompson BG, Spetzler RF (1996) The two-point method: evaluating brain stem lesions. Barrow Neurol Inst Q 12(1):1–6

5. Cavalcanti DD, Preul MC, Kalani MYS, Spetzler RF (2015) Microsurgical anatomy of safe entry zones to the brainstem. J Neurosurg:1–18
6. Epstein F, McCleary EL (1986) Intrinsic brain-stem tumors of childhood: surgical indications. J Neurosurg 64(1):11–15
7. Giliberto G, Lanzino DJ, Diehn FE, Factor D, Flemming KD, Lanzino G (2010) Brainstem cavernous malformations: anatomical, clinical, and surgical considerations. Neurosurg Focus 29(3):E9
8. Ishihara H, Bjeljac M, Straumann D, Kaku Y, Roth P, Yonekawa Y (2006) The role of intraoperative monitoring of oculomotor and trochlear nuclei -safe entry zone to tegmental lesions. Min - Minimally Invasive Neurosurgery 49(3):168–172
9. Kaku Y, Yonekawa Y, Taub E (1999) Transcollicular approach to intrinsic tectal lesions. Neurosurgery 44(2):333–343
10. Kalani MY, Yagmurlu K, Spetzler RF The interpeduncular fossa approach for resection of ventromedial midbrain lesions. J Neurosurg
11. Kyoshima K, Kobayashi S, Gibo H, Kuroyanagi T (1993) A study of safe entry zones via the floor of the fourth ventricle for brain-stem lesions. J Neurosurg 78(6):987–993
12. Lassiter KRL, Alexander E Jr, Davis CH Jr, Kelly DL Jr (1971) Surgical treatment of brain stem gliomas. J Neurosurg 34(6): 719–725
13. Matson DD, Ingraham FD (1969) Neurosurgery of infancy and childhood, 2nd edn, Springfield
14. Párraga RG, Possatti LL, Alves RV, Ribas GC, Türe U, de Oliveira E (2015) Microsurgical anatomy and internal architecture of the brainstem in 3D images: surgical considerations. J Neurosurg:1–19
15. Porter RW, Detwiler PW, Spetzler RF, Lawton MT, Baskin JJ, Derksen PT, Zabramski JM (1999) Cavernous malformations of the brainstem: experience with 100 patients. J Neurosurg 90(1): 50–58
16. Raimondi AJ (1987) Pediatric neurosurgery, 2nd edn. Springer, New York
17. Wind JJ, Bakhtian KD, Sweet JA, Mehta GU, Thawani JP, Asthagiri AR, Oldfield EH, Lonser RR (2010) Long-term outcome after resection of brainstem hemangioblastomas in von Hippel-Lindau disease. J Neurosurg 114(5):1312–1318
18. Yagmurlu K, Rhoton AL Jr, Tanriover N, Bennett JA (2014) Three-dimensional microsurgical anatomy and the safe entry zones of the brainstem. Neurosurgery 10:602–620
19. Yagmurlu K, Kalani MY, Preul MC, Spetzler RF The superior fovea triangle approach: a novel safe entry zone to the brainstem. J Neurosurg
20. Zhou LF, Du G, Mao Y, Zhang R (2005) Diagnosis and surgical treatment of brainstem hemangioblastomas. Surg Neurol 63(4): 307–315